TECHNICAL NOTE

Influence of particle shape on small-strain damping ratio of dry sands

M. PAYAN*, K. SENETAKIS*, A. KHOSHGHALB* and N. KHALILI*

This study reports on the significance of particle shape on the small-strain damping ratio of dry sands in shear ($D_{s,min}$) through a comprehensive set of torsional resonant column tests. Sands with a variety of grain shapes prepared at variable initial densities are studied. The samples are subjected to torsional resonant column tests under isotropic confining pressures (p') ranging from 50 to 800 kPa. Small-strain damping ratios are derived based on the free-vibration decay mode of the samples and the results are compared with the half-power bandwidth method. The effects of grain size distribution, particle shape and effective confining stress on $D_{s,min}$ are thoroughly discussed, and a new model for the prediction of small-strain damping ratio of dry sand is proposed.

KEYWORDS: dynamics; laboratory tests; sands

INTRODUCTION

Damping ratio in shear (D_s) is an important soil property for the geophysical characterisation of sediments, seismic design of civil engineering facilities and study of energy dissipation in geomaterials (Richart *et al.*, 1970; Cascante & Santamarina, 1996; Ishihara, 1996). At small strains, damping ratio reaches a minimum value, denoted by $D_{s,min}$. Mechanisms of energy loss at small strains are not well understood in the literature. Santamarina & Cascante (1996) reported that processes other than frictional losses are involved in the dissipation of energy at small strains. Menq (2003) and Senetakis *et al.* (2012) related $D_{s,min}$ to the mean effective confining pressure and gradation characteristics of the soil. Senetakis *et al.* (2013) discussed the influence of particle morphology on $D_{s,min}$ and attributed it to the shape descriptors of the particles. The effect of particle shape on small-strain dynamic properties has also been emphasised by Santamarina & Cascante (1998), Cho *et al.* (2006) and Payan *et al.* (2016). Nevertheless, no systematic investigation of the effect of particle shape on the damping properties of sands has to date been reported in the literature.

The main objective of this note is to report on the results of an experimental study on the effect of particle shape on the small-strain damping ratio of dry sands. For this purpose, samples of sands with a variety of grain shapes are examined in a resonant column apparatus in torsional mode of vibration to determine their small-strain damping ratio using two different approaches: free-vibration decay and half-power bandwidth methods. The analyses of the results are incorporated into a new expression for the prediction of small-strain damping ratio of sands in shear, taking into account the effects of particle shape as well as grain size characteristics.

TEST MATERIALS AND METHODS

Eleven sands with various gradations and particle shapes were tested in this study. The grading curves of the sands are presented in Fig. 1. The grain size characteristics as well as particle shape descriptors are given in Table 1. Blue and uniform Sydney sands were used for independent verification purposes and were not included in the model development. All test soils were classified as SP according to the Unified Soil Classification System (USCS) with a coefficient of curvature (C_c) close to unity. Dry samples were prepared to target void ratios in a metal split mould placed directly on the base pedestal of a resonant column apparatus (RCA) with fixed-free ends. For the data analysis, 19 samples were prepared and tested in the RCA under isotropic confining pressures, p', ranging from 50 to 800 kPa. Samples' initial void ratios, e_o, are given in Table 1. All the specimens were tested in a dry state in the torsional mode of vibration. The sequence of increasing p' adopted in the tests was 50, 100, 200, 400, 600 and 800 kPa.

The particle shape descriptors in Table 1 were quantified visually in an optical microscope adopting a widely used empirical chart proposed by Krumbein & Sloss (1963) (Fig. 2). For a given sand, 30 particles were randomly selected and two shape descriptors, namely roundness, R, and sphericity, S, were quantified. The roundness is related to the local surface features of the sand particles, and is defined as the ratio of the average radius of the surface features to the radius of the largest sphere inscribed in the sand particle. Sphericity is an indication of the general shape of sand particles and is quantified as the ratio of the radius of the largest inscribed sphere in the particle to the smallest circumscribed sphere to the particle. The definitions of R and S are shown schematically in Fig. 2. Only the mean values of R and S denoted by R (mean) and S (mean) are presented in Table 1. The regularity, ρ, was calculated as the algebraic mean of the roundness and sphericity, that is, $\rho = 0{\cdot}5 \times (R + S)$. Regularity was introduced by Cho *et al.* (2006) to simultaneously account for the effects of both roundness and sphericity in the mechanical behaviour of geomaterials. The mean value of regularity for each sample, denoted by ρ (mean), was used in the analyses in this study.

The values of small-strain damping ratio in shear were obtained using the free-vibration decay (FVD) method (ASTM, 2015) as well as the half-power bandwidth (HPB) method. In the FVD method, three successive cycles during free vibration of the samples were adopted for small-strain damping ratio calculations, as suggested by Stokoe *et al.* (1999). A typical example of the experimental results along with the calculations to obtain the small-strain damping ratio using FVD and HPB methods are given in Figs 3 and 4, respectively. Note that the measurements of small-strain damping ratio in this study

Manuscript received 16 October 2015; revised manuscript accepted 11 January 2016.
Discussion on this paper is welcomed by the editor.
* School of Civil and Environmental Engineering, UNSW Australia, Sydney, Australia.

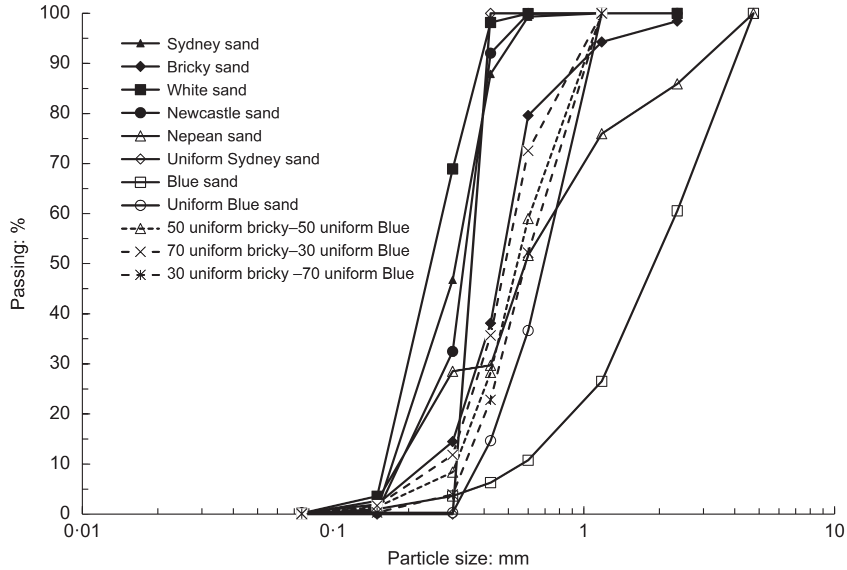

Fig. 1. Particle size distribution curves of the tested sands

Table 1. Different properties of the soils tested in the study

Laboratory material (sand)	Grading		Particle shape descriptors*			e_o†
	d_{50}‡: mm	C_u‡	R (mean)	S (mean)	ρ (mean)	
Sydney	0·31	1·95	0·61	0·76	0·69	0·66, 0·70, 0·75, 0·80, 0·85
Bricky	0·47	2·19	0·48	0·71	0·60	0·75
White (Blue circle)	0·24	1·69	0·71	0·76	0·74	0·75
Newcastle	0·33	1·94	0·64	0·73	0·69	0·75
Nepean (River)	0·59	4·15	0·55	0·77	0·66	0·75, 0·80
Uniform Sydney	0·36	1·18	0·61	0·76	0·69	0·75, 0·85
Blue	1·88	4·11	0·24	0·51	0·38	0·75
Uniform Blue	0·69	1·99	0·24	0·51	0·38	0·75, 0·80, 0·85
50% uniform bricky, 50% uniform Blue	0·54	1·96	0·36	0·61	0·49	0·75, 0·85
70% uniform bricky, 30% uniform Blue	0·49	2·01	0·41	0·65	0·53	0·75, 0·85
30% uniform bricky, 70% uniform Blue	0·59	1·99	0·31	0·57	0·44	0·75, 0·85

*Obtained according to the modified version of particle shape characterisation chart developed by Cho *et al.* (2006).
†e_o, initial void ratio.
‡d_{50}, mean grain size; $C_u = d_{60}/d_{10}$.
R, roundness; S, sphericity; ρ, regularity.

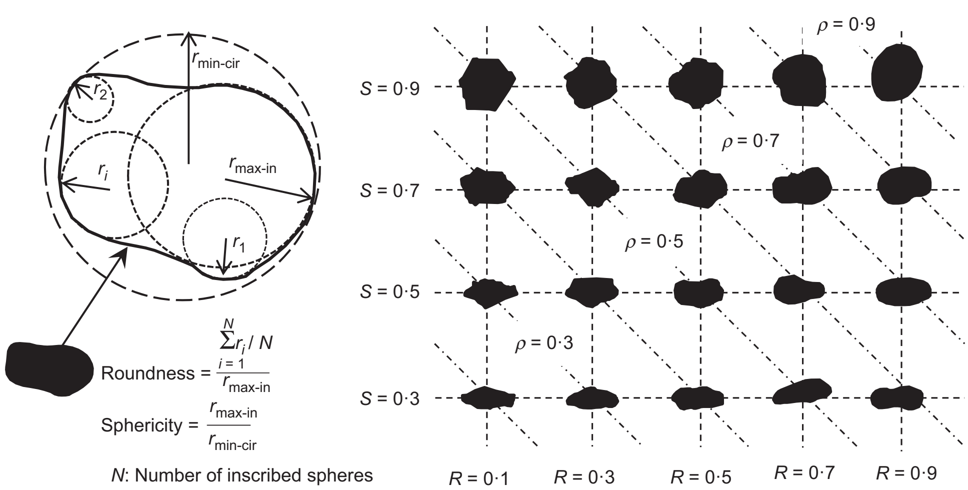

Fig. 2. Particle shape characterisation chart (Krumbein & Sloss, 1963; Cho *et al.*, 2006)

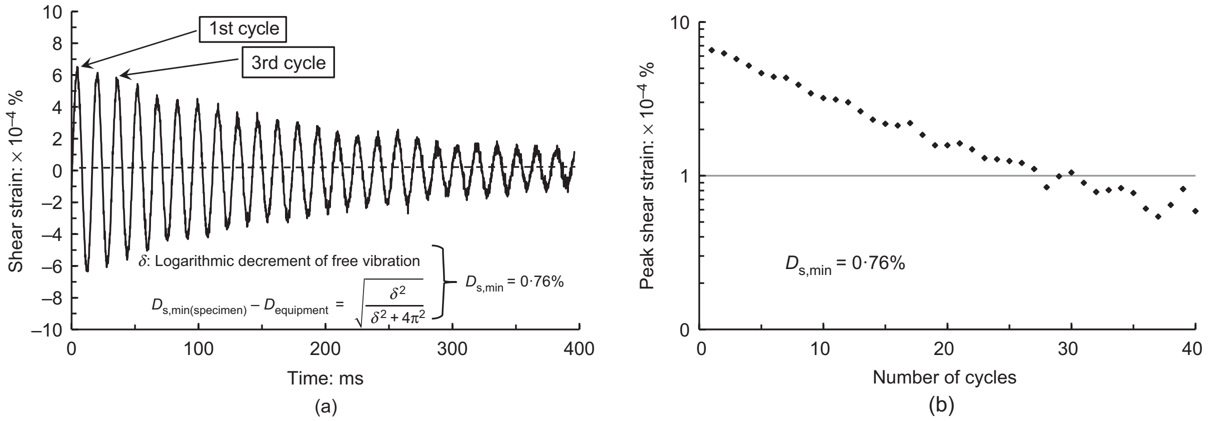

Fig. 3. Typical test results and calculations based on FVD method for the estimation of small-strain damping ratio; dry Sydney sand; $e_o = 0{\cdot}8$, $p' = 100$ kPa

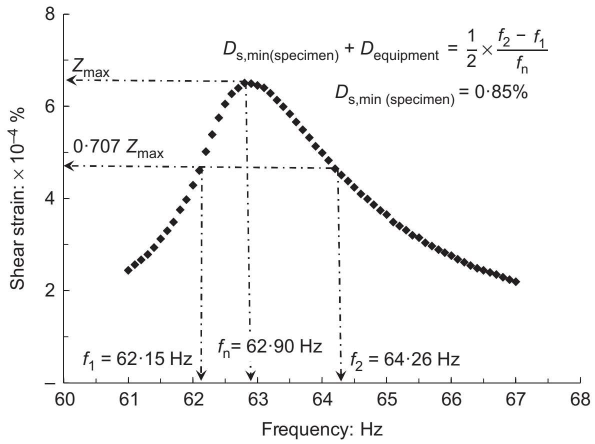

Fig. 4. Typical test results and calculations based on HPB method for the estimation of small-strain damping ratio; dry Sydney sand; $e_o = 0{\cdot}8$, $p' = 100$ kPa

corresponded to shear strain amplitudes less than $10^{-3}\%$ and thus the behaviour falls within the linear-elastic range (Oztoprak & Bolton, 2013). Comparisons between the results from FVD and HPB methods were conducted for all the tests and the results are illustrated in Fig. 5. Within the scatter of the data, the two methods provide reasonably similar small-strain damping ratio values, which is in agreement with the recent work by Senetakis *et al.* (2015). Small-strain damping ratios obtained using the FVD method were used for the model development and verification in this study.

RESULTS AND DISCUSSION

Typical test results in terms of the variation of small-strain damping ratio, $D_{s,min}$, plotted against the effective confining pressure, p', normalised with respect to the atmospheric pressure, p_a, for different particle shapes, but similar initial void ratios, are presented in Fig. 6. As previously observed by Menq (2003) and Senetakis *et al.* (2012, 2013), among others, the results show $D_{s,min}$ decreases with increasing isotropic confining pressure. However, more importantly, they show a strong dependency of $D_{s,min}$ on the shape descriptor ρ, particularly at the lower ratios of p'/p_a.

In order to isolate more clearly the influence of particle shape on small-strain damping ratio, the effects of gradation must be excluded from the observed trends in Fig. 6. To this end, the authors note that the small-strain damping ratio is not influenced by the soil density or the void ratio (Santamarina & Cascante, 1998), and that $D_{s,min}$ is related to p'/p_a in the form of a power law as (Menq, 2003; Senetakis *et al.*, 2012, 2013)

$$D_{s,min} = C \times \left(\frac{p'}{p_a}\right)^{\kappa} \tag{1}$$

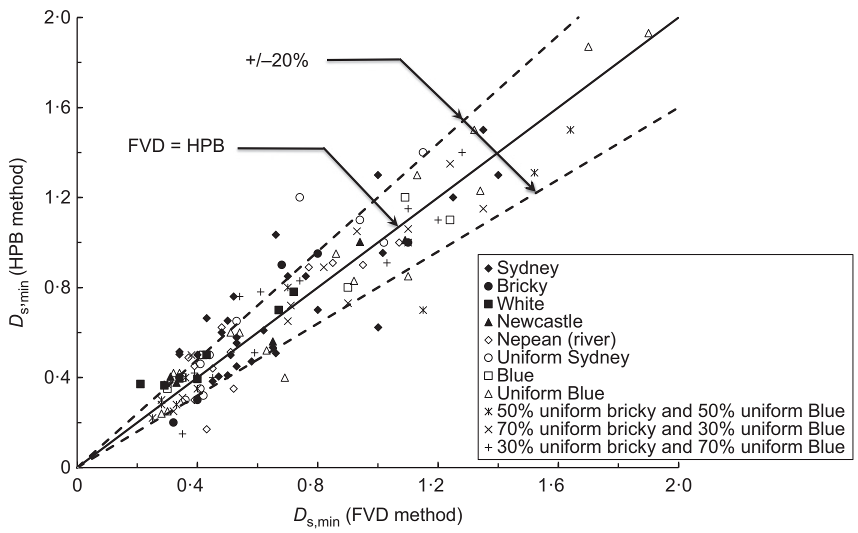

Fig. 5. Comparison between FVD and HPB methods for calculations of small-strain damping ratio

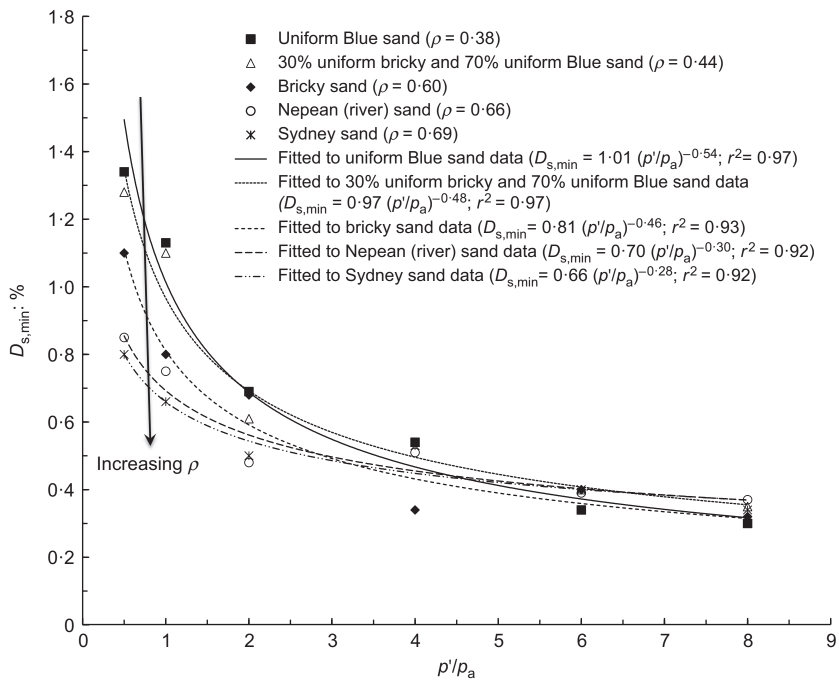

Fig. 6. Variation of small-strain damping ratio with normalised confining pressure for five tested sands with initial void ratio of 0·75

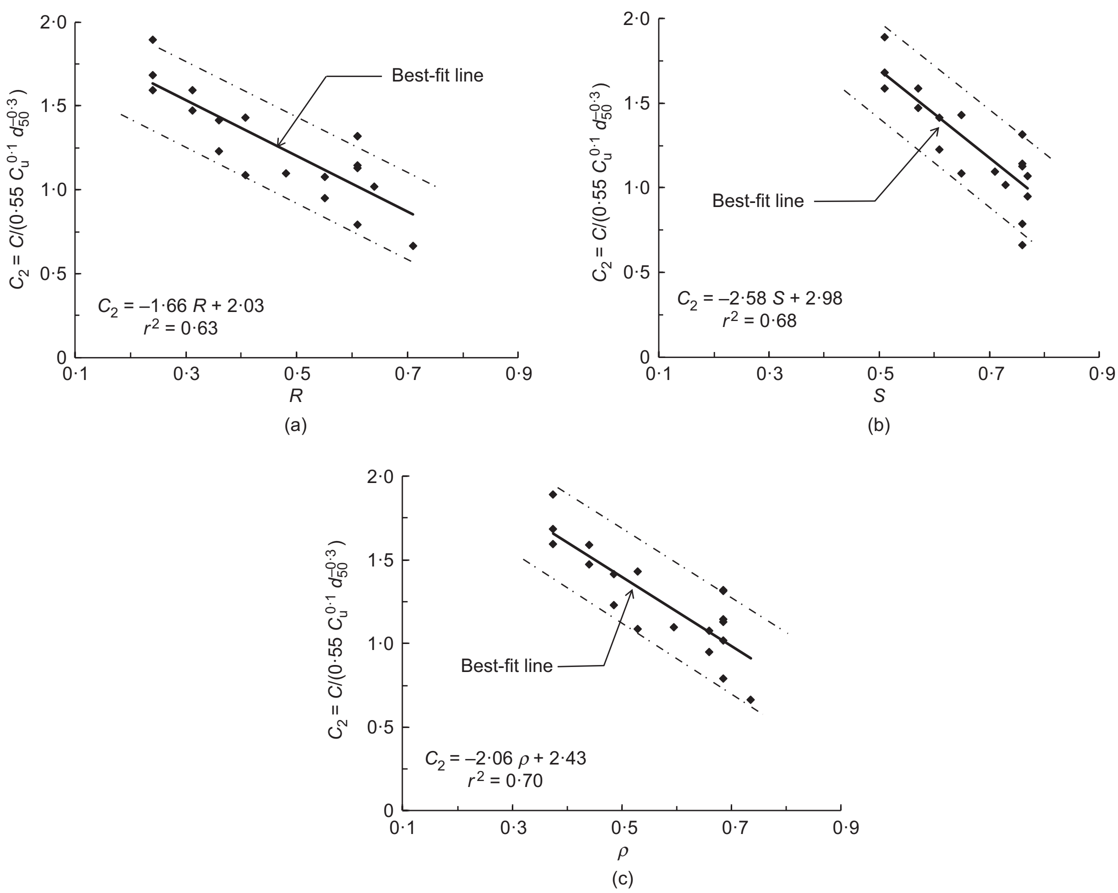

Fig. 7. Variation of normalised *C* with different shape descriptors: (a) roundness; (b) sphericity; (c) regularity

where C and κ are material parameters, which a priori may be considered functions of gradation and particle shape of the soil. However, based on the work of Menq (2003), and Senetakis *et al*. (2012, 2013), exponent κ is not influenced by gradation. Therefore, it is assumed in this work that κ is only a function of particle shape, but C is affected by both grain size characteristics and particle shape as

$$C = C_1(\text{grain size characteristics}) \times C_2(\text{particle shape}) \tag{2}$$

in which C_1 captures the effect of gradation and C_2 is a function of particle shape. Menq (2003) proposed the following expression for C_1

$$C_1 = 0{\cdot}55 \times C_u^{0{\cdot}1} \times d_{50}^{-0{\cdot}3} \tag{3}$$

where C_u and d_{50} are the coefficient of uniformity and the mean grain size (in mm), respectively. Adopting equation (1), parameters C and κ can be obtained for each test soil from the best fits to the experimental data shown in Fig. 6. C_2 can then be extracted from C using equations (2) and (3).

Variations of C_2 and κ for the test soils against the shape descriptors R, S and ρ are shown in Figs 7 and 8. For both parameters, within the scatter of data, the systematic effect of particle shape can be observed. Linear best fits to the experimental data (using the minimum least-square error

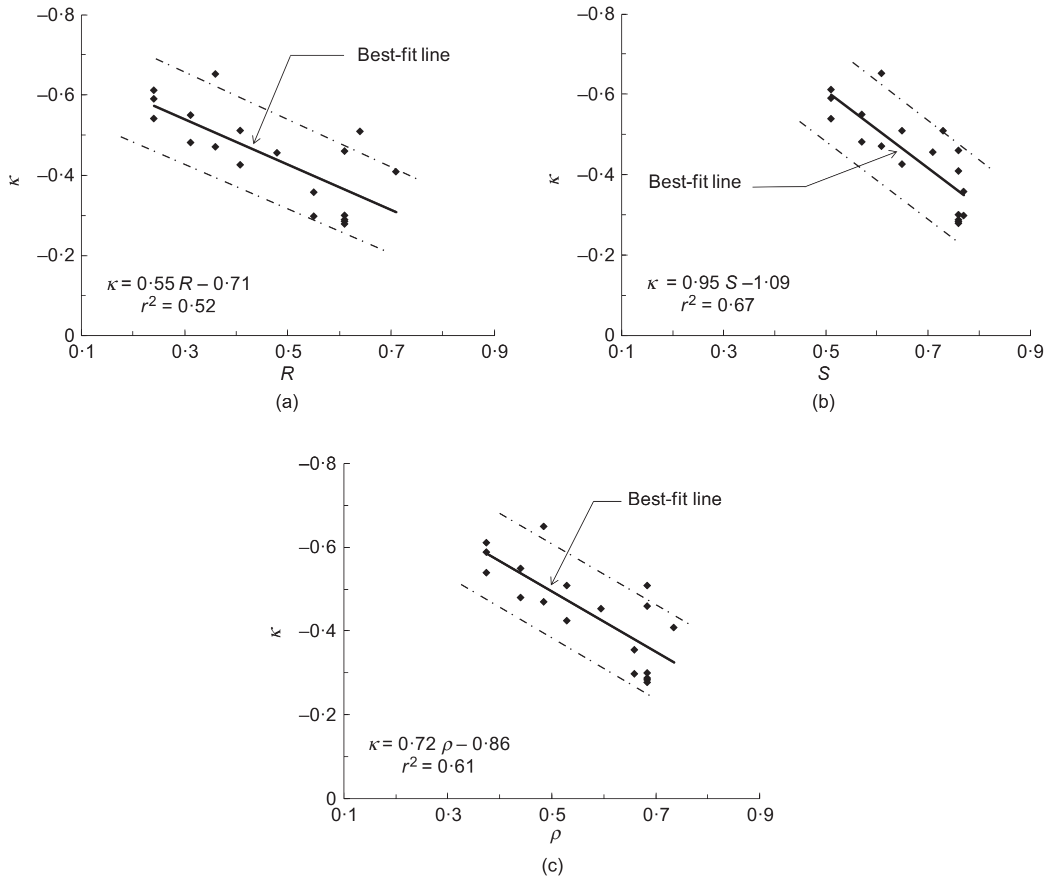

Fig. 8. Variation of κ with different shape descriptors: (a) roundness; (b) sphericity; (c) regularity

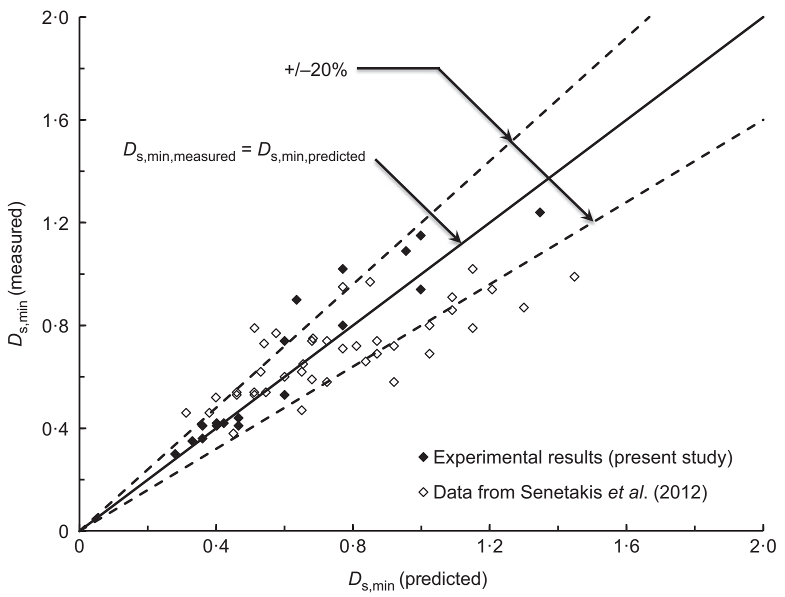

Fig. 9. Comparison between measured and predicted values of small-strain damping ratio

method) along with the corresponding coefficients of correlation (r^2) are also depicted in Figs 7 and 8. As can be seen, the absolute value of exponent κ decreases with an increase in regularity. This observation is in quantitative agreement with the work by Senetakis *et al.* (2012) on dry granular soils, implying that the effect of confining pressure on $D_{s,min}$ becomes less prominent for sands with increasing value of regularity, ρ. Similarly, parameter C_2 decreases as regularity increases, an aspect which has been neglected in the previous studies of small-strain damping ratio.

A NEW MODEL OF $D_{s,min}$ INCLUDING PARTICLE SHAPE

Considering the similar effects of S and R on C_2 and κ (Figs 7 and 8), regularity, ρ, is deemed to be an effective parameter to incorporate the effect of particle shape on small-strain damping ratio in this study. Thus, based on the best fits in Figs 7(c) and 8(c), and equations (1)–(3), an expression for small-strain damping ratio of sands including the effects of particle shape and gradation may be proposed as follows

$$D_{s,min} = \left(0{\cdot}55 \times C_u^{0{\cdot}1} \times d_{50}^{-0{\cdot}3}\right) \times (-2{\cdot}06\rho + 2{\cdot}43) \times \left(\frac{p'}{p_a}\right)^{0{\cdot}72\rho - 0{\cdot}86} \tag{4}$$

To explore the validity of equation (4), measured against predicted values of $D_{s,min}$ are plotted in Fig. 9 for three independent sets of tests: uniform Sydney sand with two initial void ratios of 0·75 and 0·85, and Blue sand with the initial void ratio of 0·75. Also presented in Fig. 9 are the damping ratio data reported by Senetakis *et al.* (2012) plotted against the predicted values from equation (4). For the data by Senetakis *et al.* (2012), regularity (ρ) values of 0·5 and 0·7 were reported for crushed sand and river sand, respectively. Considering the difficulties in measuring damping ratio at small strains, and the extensive scatter in the data that is reported in the literature, a very good comparison between measured and predicted values of $D_{s,min}$ is obtained for all practical purposes.

CONCLUDING REMARKS

A set of resonant column tests has been performed with a focus on the determination of the small-strain damping ratio of dry sands using two different approaches: free-vibration decay and half-power bandwidth methods. Using systematic normalisations, the effect of particle shape is isolated and incorporated into the development of a new expression for determination of small-strain damping ratio for sands subject to isotropic confining stress. Particle shape is expressed by means of regularity, which is the average of two particle shape descriptors: the roundness and the sphericity. Comparisons of predicted values of small-strain damping ratio based on the new model and the data reported in this study, and also in the literature, demonstrate a satisfactory performance of the new model.

NOTATION

C	material parameter related to small-strain damping ratio
C_c	coefficient of curvature
C_u	coefficient of uniformity
C_1	material parameter describing the contribution function of grain size characteristics in small-strain damping ratio of sand
C_2	material parameter describing the contribution function of particle shape in small-strain damping ratio of sand
$D_{equipment}$	damping of equipment
D_s	damping ratio in shear
$D_{s,min}$	small-strain damping ratio in shear
$D_{s,min(specimen)}$	small-strain damping ratio in shear of specimen
$D_{s,min,measured}$	measured small-strain damping ratio in shear
$D_{s,min,predicted}$	predicted small-strain damping ratio in shear
d_{10}	grain diameter at 10% passing
d_{50}	mean grain size of sand
d_{60}	grain diameter at 60% passing
e_o	initial void ratio
f_n	natural resonant frequency
f_1, f_2	frequencies corresponding to 0·707 times the maximum shear strain amplitude of vibration
N	number of inscribed spheres in sand particle
p'	isotropic confining pressure
p_a	atmospheric pressure
R	roundness
$r_{max\text{-}in}$	radius of largest sphere inscribed in sand particle
$r_{min\text{-}cir}$	radius of smallest sphere circumscribed to sand particle
$r_1, r_2, \ldots, r_i$	radius of spheres inscribed in sand particle
r^2	coefficient of correlation
S	sphericity
Z_{max}	maximum shear strain amplitude of vibration
δ	logarithmic decrement of free vibration
κ	material parameter related to small-strain damping ratio as a function of particle shape
ρ	regularity

REFERENCES

ASTM (2015). D4015-15: Standard test methods for modulus and damping of soils by fixed-base resonant column devices. West Conshohocken, PA, USA: ASTM International.

Cascante, G. & Santamarina, C. (1996). Interparticle contact behavior and wave propagation. *J. Geotech. Geoenviron. Engng, ASCE* **122**, No. 10, 831–839.

Cho, G. C., Dodds, J. & Santamarina, J. C. (2006). Particle shape effects on packing density, stiffness, and strength: natural and crushed sands. *J. Geotech. Geoenviron. Engng* **132**, No. 5, 591–602.

Ishihara, K. (1996). *Soil behaviour in earthquake geotechnics.* Oxford, UK: Oxford University Press.

Krumbein, W. C. & Sloss, L. L. (1963). *Stratigraphy and sedimentation*, 2nd edn. San Francisco, CA, USA: Freeman and Company.

Menq, F.Y. (2003). *Dynamic properties of sandy and gravelly soils.* PhD dissertation, University of Texas, Austin, TX, USA.

Oztoprak, S. & Bolton, M. D. (2013). Stiffness of sands through a laboratory test database. *Géotechnique* **63**, No. 1, 54–70, http://dx.doi.org/10.1680/geot.10.P.078.

Payan, M., Khoshghalb, A., Senetakis, K. & Khalili, N. (2016) Effect of particle shape and validity of G_{max} models for sand: a critical review and a new expression. *Comput. Geotech.* **72**, 28–41.

Richart, F. E., Hall, J. R. & Woods, R. D. (1970). *Vibrations of soils and foundations.* Englewood Cliffs, NJ, USA: Prentice Hall.

Santamarina, C. & Cascante, G. (1996). Stress anisotropy and wave propagation: a micromechanical view. *Can. Geotech. J.* **33**, 770–782.

Santamarina, C. & Cascante, G. (1998). Effect of surface roughness on wave propagation parameters. *Géotechnique* **48**, No. 1, 129–136, http://dx.doi.org/10.1680/geot.1998.48.1.129.

Senetakis, K., Anastasiadis, A. & Pitilakis, K. (2012). The small-strain shear modulus and damping ratio of quartz and volcanic sands. *Geotech. Test. J.* **35**, No. 6, 1–17.

Senetakis, K., Anastasiadis, A. Pitilakis, K. & Coop, M. (2013). The dynamics of a pumice granular soil in dry state under isotropic resonant column testing. *Soil Dynam. Earthquake Engng* **45**, 70–79.

Senetakis, K., Anastasiadis, A. & Pitilakis, K. (2015). A comparison of material damping measurements in resonant column using the steady-state and free-vibration decay methods. *Soil Dynam. Earthquake Engng* **74**, 10–13.

Stokoe, K., Darendeli, M., Andrus, R. & Brown, L. T. (1999). Dynamic soil properties: laboratory, field and correlation studies. *Proceedings of the 2nd international conference on earthquake geotechnical engineering*, Lisbon, Portugal, pp. 811–845.